HUMAN GENE THERAPY 12:2051–2063 (November 20, 2001)
Mary Ann Liebert, Inc.

Blocking Caspase-Activated Apoptosis Improves Contractility in Failing Myocardium

KARL-LUDWIG LAUGWITZ,[1]* ALESSANDRA MORETTI,[1]* HANS-JÖRG WEIG,[1]*
ANGELIKA GILLITZER,[1] KAI PINKERNELL,[1] THOMAS OTT,[1] INGO PRAGST,[2]
CHRISTIAN STÄDELE,[2] MELCHIOR SEYFARTH,[1] ALBERT SCHÖMIG,[1] and MARTIN UNGERER[3]

ABSTRACT

Cardiac myocyte apoptosis has been demonstrated in end-stage failing human hearts. The therapeutic utility of blocking apoptosis in congestive heart failure (CHF) has not been elucidated. This study investigated the role of caspase activation in cardiac contractility and sarcomere organization in the development of CHF. In a rabbit model of heart failure obtained by rapid ventricular pacing, we demonstrate, using *in vivo* transcoronary adenovirus-mediated gene delivery of the potent caspase inhibitor p35, that caspase activation is associated with a reduction in contractile force of failing myocytes by destroying sarcomeric structure. In this animal model gene transfer of p35 prevented the rise in caspase 3 activity and DNA–histone formation. Genetically manipulated hearts expressing p35 had a significant improvement in left ventricular pressure rise (+*dp/dt*), decreased end-diastolic chamber pressure (LVEDP), and the development of heart failure was delayed. To better understand this benefit, we examined the effects of caspase 3 on cardiomyocyte dysfunction *in vitro*. Microinjection of activated caspase 3 into the cytoplasm of intact myocytes induced sarcomeric disorganization and reduced contractility of the cells. These results demonstrate a direct impact of caspases on cardiac function and may lead to novel therapeutic strategies via antiapoptotic regimens.

OVERVIEW SUMMARY

In human ischemic and dilated cardiomyopathy, activation of the caspase cascade has been documented. This study investigated the role of caspase activation in cardiac contractility and sarcomere organization in the development of CHF. In a rabbit model of heart failure adenovirus-mediated gene delivery of the potent caspase inhibitor p35 improved ventricular function assessed by echocardiographic and hemodynamic measurements. Failing cardiomyocytes isolated from genetically manipulated hearts expressing p35 showed preserved sarcomeric structure and reconstituted contractile performance. Microinjection of caspase 3 into healthy myocytes induced a concentration-dependent destruction of the sarcomeric units and reduced contractility of the cells. These data provide evidence that caspase activation contributes to the progression of CHF and its prevention leads to partial restoration of cardiac function.

INTRODUCTION

DESPITE PROGRESS in the treatment of heart failure, the 5-year mortality of symptomatic patients still exceeds 50% (Braunwald and Bristow, 2000). Histochemical evidence of apoptosis has been identified in several cardiovascular disorders leading to congestive heart failure, including ischemic heart disease, myocarditis, and dilated cardiomyopathy (Haunstetter and Izumo, 2000; MacLellan, 2000). In cardiomyocytes, programmed cell death may be an important component of the transition from adaptive hypertrophy to heart failure (Hirota *et al.*, 1999; Hunter and Chien, 1999). Prolonged growth stimulation of adult cardiomyocytes, which differentiate and withdraw from the cell cycle during the neonatal period, may activate the apoptotic program and lead to cell dysfunction in congestive heart failure (CHF).

Myocardial apoptosis involves highly complex, regulated cell suicide machinery, in which two main signaling pathways lead to activation of the caspase family of cysteine proteases

[1]Medizinische Klinik and Deutsches Herzzentrum München, 81675 Munich, Germany.
[2]Institut für Experimentelle Onkologie und Therapieforschung, Technische Universität München, 81675 Munich, Germany.
[3]ProCorde GmbH, 82152 Martinsried-Munich, Germany.
*Karl-Ludwig Laugwitz, Alessandra Moretti, and Hans-Jörg Weig contributed equally to this work.

(Reed and Paternostro, 1999; Hengartner, 2000): (1) death receptor signaling (e.g., Fas, tumor necrosis factor [TNF], and DR3-DR5 receptors) (Ashkenazi and Dixit, 1998) and (2) release of cytochrome *c* from mitochondria and subsequent *trans*-activation of procaspase 9 by apoptosis protease-activating factor (Apaf) (Green and Reed, 1998). Caspases regulate the execution of the mammalian cell death program (Hengartner, 2000). Caspase 3 represents the key effector enzyme and cleaves downstream targets involved in the expression of the apoptotic phenotype, including gelsolin, p21-activated kinase 2 (PAK2), nuclear lamins, and the inhibitory subunit of DNA fragmentation factor (inhibitor of caspase-activated DNase, ICAD) (Rudel and Bokoch, 1997; Enari *et al.*, 1998). In human ischemic and dilated cardiomyopathy, cytochrome *c* release and activation of the caspase 3 cascade have been documented (Narula *et al.*, 1999). Critical questions remain unclear: to what extent do caspases contribute to functional deterioration of cardiomyocytes in failing myocardium and can we develop effective new therapies based on the blockade of apoptotic pathways in the myocardium? As cytoskeletal proteins (e.g., gelsolin, actin, and fodrin) are important targets for activated caspase 3 (Hengartner, 2000), abnormal cytoskeletal structure or loss of sarcomere organization through caspases could lead to abnormalities in myocyte function and decreased force transmission.

The goal of this study was to investigate the role of caspase activation in cardiac contractility and sarcomere organization in the development of heart failure. We tested whether expression of p35, which potently inhibits members of the caspase family of cysteine proteases (Bump *et al.*, 1995), can improve ventricular function in an animal model of heart failure. In failing myocardium, we analyzed caspase 3, caspase-activated deoxyribonuclease (CAD) activities, and DNA fragmentation over the time course of heart failure development. Two days after pacemaker implantation, rabbits were randomized to receive either a bicistronic adenovirus carrying p35 and green fluorescent protein genes (CHF+Ad-p35) or GFP alone (CHF+Ad-GFP) by using a transcoronary gene delivery technique. After 0, 7, and 15 days of rapid pacing, echocardiographic and hemodynamic profiles of the animals were analyzed. To address specifically the molecular mechanism that mediates the caspase-induced deterioration of cardiac performance, we studied the effects of microinjected caspase 3, as principal enzyme of the caspase cascade, on sarcomeric structure and contractile force in isolated ventricular cardiomyocytes.

MATERIALS AND METHODS

Construction and purification of recombinant adenovirus

Recombinant (E1- and E3-deficient) adenovirus (serotype 5) carrying the baculovirus apoptotic suppressor p35 was generated as described (He *et al.*, 1998). The coding sequence of p35 was tagged with the FLAG epitope and inserted into the polylinker sequence of the GFP-expressing pAdTrack vector, between a non-tissue-specific cytomegalovirus (CMV) promoter and a simian virus 40 (SV40) polyadenylation signal. Recombinant adenoviruses were prepared at large scale as described (Laugwitz *et al.*, 1999). Adenoviral titers were determined by plaque titration on HEK 293 cells.

Experimental protocol

The project was approved by the institutional ethics review board. Sixty-three adult male New Zealand White rabbits (2.8 ± 0.5 kg) were initially randomized in two groups: one group of 40 animals with implantation of pacemakers and rapid ventricular pacing and a second group of 23 sham-operated animals with implantation of pacing wires but no pacing. All animals survived the initial operation. In the first group, 18 rabbits received an intracoronary infusion of Krebs-Ringer solution, and were paced for 7 ($n = 7$) or 15 ($n = 11$) days. These animals served as failing rabbits (CHF) for hemodynamic evaluation and apoptotic biochemistry for caspase 3 activity, CAD activity, TUNEL (TdT [terminal deoxynucleotidyl-transferase]-mediated dUTP nick end labeling) staining, and DNA–histone formation. In the other 22 animals of this group, transcoronary delivery of recombinant adenoviruses encoding either p35 and GFP (CHF+Ad-p35; $n = 10$) or GFP alone (CHF+Ad-GFP; $n = 12$) was performed, and the rabbits were paced for 15 days. The second group of 23 sham-operated animals received intracoronary Krebs-Ringer solution (sham; $n = 11$), Ad-p35 (sham+Ad-p35; $n = 4$), and Ad-GFP (sham+Ad-GFP; $n = 8$). These animals were used to examine the expression levels of p35 and GFP 0, 4, 7, and 15 days after infection and for apoptotic biochemistry, TUNEL staining, single-cell shortening, confocal laser scanning microscopy, and microinjection experiments.

In vivo *transcoronary gene delivery*

Of the 22 rabbits with ventricular pacing and adenoviral gene transfer, 2 animals in the CHF+Ad-p35 group and 4 in the CHF+Ad-GFP group died during the gene delivery procedure (in each group 8 animals survived). Rabbits were anesthetized intramuscularly with medetomidin (100 μg/kg), propofol (5 μg/kg per hr), and a bolus of fentanyl (10 μg/kg) intravenously. They were intubated, ventilated, and monitored for electrocardiogram (ECG), echocardiography, and pressure throughout the experiment. Transcoronary gene delivery into the rabbit myocardium was performed at the time ventricular pacing was initiated, 2 days after pacemaker implantation. All animals enrolled in the study received a 2-min intracoronary infusion of serotonin (10 μ*M*) and low calcium (1.25 m*M*) into the left coronary ostium, followed by a total dose of 5×10^{10} PFU of adenovirus (Weig *et al.*, 2000). In eight animals of the CHF+Ad-p35 and CHF+Ad-GFP groups hemodynamic and echocardiographic experiments were performed. All animals were killed 15 days after gene delivery and hearts were collected for biochemical studies, single-cell shortening experiments, and phalloidin staining.

Pacemaker implantation

The pacemaker lead (2F; Medtronic, Unterschleiβheim, Germany) was placed through the jugular vein into the right ventricular apex. Customized pacemakers (Vitatron, Cologne, Germany) were placed beneath the left epigastrium and connected to the lead. Sham-operated animals had the same intervention with implantation of pacing wires but never underwent initiation of ventricular pacing. Two days after surgery, ventricular pacing was initiated at a rate of 340 beats/min.

In vivo *hemodynamic and echocardiographic measurements*

Left ventricular (LV) contractility was examined before and 7 and 15 days after adenoviral gene transfer and initiation of pacing. Rabbits were anesthetized as described previously. Transthoracic M-mode and two-dimensional echocardiography was performed with a 5-MHz probe of a Hewlett-Packard (Palo Alto, CA) Sonos 5500 imaging system, as described in previous studies (Gardin *et al.*, 1995), and analyzed by two blinded observers. After preparation of the right carotid artery, a Millar 2.5F tip catheter connected to a differentiating device (Hugo Sachs, Freiburg, Germany) was placed in the left ventricle. After definition of basal contractility and LV pressure (with the pacemaker turned off), 200 μl of 0.9% NaCl was injected as a negative control. After a sufficient equilibration period, epinephrine was injected in concentrations ranging from 0.1 to 0.8 μg/kg per min.

Preparation and culture of rat and rabbit adult ventricular cardiomyocytes

Single ventricular myocytes were isolated from male Wistar rats (250–300 g) or from sham-operated and failing male New Zealand White rabbits (2.8 ± 0.5 kg), as described (Laugwitz *et al.*, 1999). Cardiomyocytes were cultured in M199 culture medium (supplemented with minimal essential medium [MEM] vitamins, MEM nonessential amino acids, 25 m*M* HEPES, insulin [10 μg/ml], penicillin [100 IU/ml], streptomycin [100 μg/ml], and gentamicin [100 μg/ml]) on laminin-precoated dishes (5 $\mu g/cm^2$; density of 10^5 cells/cm^2) in a humidified atmosphere (5% CO_2) at 37°C. Infection of rat myocytes with adenoviruses was performed *in vitro* at a multiplicity of infection (MOI) of 100 PFU/cell 6–8 hr after plating in M199 medium. Rat cells were used for biochemistry 48 hr after infection. Rabbit cardiomyocytes were infected *in vivo* and isolated 4, 7, or 15 days after gene transfer.

Western blot analysis

Immunodetection was performed in crude extracts of sham-operated and failing myocardium. Extracts were obtained by homogenization in 10 m*M* HEPES buffer, pH 7.0, containing a mixture of protease inhibitors at 4°C. Protein concentrations were detected by Bradford assay (Bio-Rad Laboratories, Munich, Germany). Equal amounts of protein (150 μg) were size fractionated on a 12% sodium dodecyl sulfate (SDS)-polyacrylamide gel and electrophoretically transferred to nitrocellulose membrane (Bio-Rad Laboratories). Blots were stained with Ponceau red, in order to monitor the amount of transferred protein in each lane and to detect protein degradation. Native ICAD cleavage products in lysates of sham-operated and failing myocardium were detected with a goat polyclonal antibody directed against the N terminus of the mouse ICAD (1:1000 dilution; Santa Cruz Biotechnology, Santa Cruz, CA). Extracts from sham-operated hearts were also incubated for 30 min at 37°C with recombinant human active caspase 3 (1 ng/μl; Becton Dickinson, Heidelberg, Germany), in the presence or absence of the tetrapeptide caspase 3 inhibitor DEVD-FMK (Asp-Glu-Val-Asp-*O*-methyl-fluoromethylketone, 100 μM). Immunodetection of p35 and α-sarcomeric actin in extracts of transcoronary-infected sham+Ad-p35 myocardium was performed with mouse anti-FLAG M2 monoclonal antibody (1:1000 dilution; Stratagene, La Jolla, CA) and mouse anti-α-sarcomeric actin monoclonal antibody (1:5000 dilution; Sigma, Munich, Germany). Antigen–antibody complexes were visualized by chemiluminescence (enhanced chemiluminescence [ECL] detection kit; Amersham Pharmacia Biotech Europe, Freiburg, Germany) and obtained chemiluminograms were evaluated by laser scanning densitometry.

Immunofluorescence staining

To determine transgene expression in transcoronary Ad-p35-infected rabbit hearts 4 days after gene delivery, frozen slices (thickness, 3 μm) were fixed in 4% paraformaldehyde and permeabilized with 0.1% saponin. p35 was detected with anti-FLAG M2 antibody (10 μg/ml) and anti-mouse IgG–Texas Red conjugate (4 μg/ml).

Polymerized actin fibers were visualized in isolated cardiomyocytes by Texas Red–phalloidin (Molecular Probes, Eugene, OR), according to the manufacturer instructions.

α-Sarcomeric actin immunodetection was performed in TUNEL-stained heart sections, using anti-α-sarcomeric actin monoclonal antibody (1:250 dilution; Sigma) and anti-mouse IgG–Texas Red conjugate (4 μg/ml).

Flow cytometry studies

Fluorescence-activated cell sorting (FACS) analysis was performed on a FACSCalibur with CellQuest software (Becton Dickinson). Cardiomyocytes freshly isolated 0, 4, 7, and 15 days after transcoronary gene delivery of Ad-GFP in sham-operated rabbits were resuspended in phosphate-buffered saline (PBS) and analyzed by flow cytometry at 520 nm (GFP fluorescence). In each measurement 2×10^4 cells were analyzed and myocytes presenting a fluorescence intensity higher than 10^1 were considered GFP positive (GFP fluorescence cutoff [M1]).

Detection of apoptosis

The activity of caspase 3 was determined with a colorimetric CPP32 assay kit by the detection of chromophore *p*-nitroanilide after cleavage of the labeled substrate DEVD-*p*-nitroanilide (Clontech, Heidelberg, Germany). A total of 2×10^6 isolated rat cardiomyocytes in culture or 50 slices from the anterolateral wall of rabbit LV myocardium (7 μm) were lysed and equal amounts of protein were reacted with 50 μM DEVD-*p*-nitroanilide at 37°C for 1 hr. The activity was determined photometrically at 405 nm, and the results were calibrated with known concentrations of *p*-nitroanilide. The units of protease activity were defined as the amount of caspase 3 required to produce 1 pmol of *p*-nitroanilide at 25°C.

CAD activity was determined by DNA fragmentation assay, using rat liver nuclei (Enari *et al.*, 1998). Briefly, 100 μg of protein from crude lysate of sham-operated or failing rabbit heart tissue was incubated with 10^6 liver nuclei in a reaction buffer consisting of 10 m*M* HEPES (pH 7.0), 40 m*M* β-glycerophosphate, 50 m*M* NaCl, 2 m*M* $MgCl_2$, 5 m*M* EGTA, 1 m*M* dithiothreitol (DTT), 2 m*M* ATP, 10 m*M* creatine phosphate, creatine kinase (50 μg/ml), and a mixture of protease inhibi-

tors. After 90 min of incubation at 37°C nuclei were lysed in 100 m*M* Tris-HCl (pH 8.5), 5 m*M* EDTA, 0.2 *M* NaCl, 0.2% SDS, and proteinase K (1 mg/ml) for 10 min at 56°C. DNA was precipitated by adding an equal volume of isopropanol, dissolved in 20 μl of Tris-HCl, pH 8.5, containing 1 m*M* EDTA and RNase A (1 mg/ml) and incubated at 37°C for 30 min. DNA was analyzed by gel electrophoresis.

TUNEL staining was performed with an *in situ* cell death detection kit (Roche Diagnostics, Mannheim, Germany) according to the manufacturer instructions, and combined with Hoechst 33258 (0.5 μg/ml; Sigma) nuclear counterstaining. Total and TUNEL-positive nuclei were counted in 10 microscopic fields from 7-μm ventricular sections for each heart. The mean number of nuclei per millimeter squared was multiplied by the section area to calculate the number of total and TUNEL-positive nuclei for each section. More than 1000 nuclei were counted for each section.

Histone-associated DNA fragments in rat ventricular cardiomyocytes and rabbit heart slices were determined with a commercially available quantitative nucleosome enzyme-linked immunosorbent assay (ELISA), according to the manufacturer instructions (Roche). The amount of nucleosomes in the lysate of 2×10^3 cells or 5 slices from the anterolateral wall of the LV (7 μm) was photometrically determined at 405 nm. The DNA fragmentation enhancement factor was calculated for each group of experiments as $OD_{treatment}/OD_{control}$, after subtraction of background OD_{405}.

Cell shortening experiments in vitro

Fractional shortening was measured in rabbit adult cardiomyocytes isolated from the LV of sham-operated or failing hearts 15 days after transcoronary adenovirus application and maintained for 1 day in culture. Experiments were performed in a temperature-controlled cuvette (37°C), at constant medium flow and constant electrical field, using an electro-optical monitoring system (Scientific Instruments, Heidelberg, Germany), as described (Laugwitz *et al.*, 1999). As medium, a 1.8 m*M* Ca^{2+}-Tyrode's solution was used. Infected cells were selected by GFP fluorescence.

Microinjection

Microinjection experiments were performed with freshly isolated myocytes from sham-operated rabbits, using a Femto-Jet microinjector (Eppendorf, Hamburg, Germany). Fluorescein isothiocyanate (FITC)-conjugated dextran (6 mg/ml) alone or plus human recombinant active caspase 3 (4 and 20 ng/μl) in 5 m*M* potassium phosphate buffer (pH 7.4, 100 m*M* KCl) was injected (P_i = 1000 hPa, t_i = 0.1 sec, P_c = 30 hPa) into the cytoplasm of cells in culture medium supplemented with 200 μ*M* 2,3-butanedione 2-monoxime (BDM), 10 μ*M* verapamil, and optionally with 100 μ*M* DEVD-FMK. After 2 hr of incubation, cells were used for contractility measurements or phalloidin staining. Injected cells were selected by FITC fluorescence.

Assessment of inflammation and necrosis

Hematoxylin–eosin staining was used to detect inflammatory cell infiltrates and necrosis in samples from LV myocardium of animals that had received adenoviral gene transfer (CHF+Ad-p35, n = 3; CHF+Ad-GFP, n = 3) after 15 days of pacing. Three CHF animals served as controls.

Statistical analysis

Data represent means ± SEM and were analyzed by one-way analysis of variance (ANOVA) followed by Scheffé post-hoc analysis. Statistical significance was accepted at the level of $p < 0.05$.

RESULTS

Effects of chronic tachycardia in rabbits

The present study investigates a model of low-output CHF that resembles human alterations at the hemodynamic and biochemical levels (Masaki *et al.*, 1993; Akhter *et al.*, 1997). Fifteen days of ventricular pacing at rates of 340 beats/min resulted in gross clinical evidence of systemic heart failure in the animals, including biventricular dilatation, pleural effusions, and abdominal ascites. Echocardiographic studies showed an

TABLE 1. ECHOCARDIOGRAPHIC AND HEMODYNAMIC MEASUREMENTS IN RABBITS AFTER 15 DAYS OF VENTRICULAR PACING AND TRANSCORONARY GENE DELIVERY OF Ad-GFP[a]

	Krebs-Ringer (n = 8)			*Ad-GFP (n = 8)*		
	Prepacing	*Postpacing*	p *Value*	*Prepacing*	*Postpacing*	p *Value*
HR, bpm	182 ± 6.0	189 ± 7.0	NS	180 ± 7.0	190 ± 10.0	NS
Body weight, kg	2.8 ± 0.5	2.75 ± 0.8	NS	2.85 ± 0.4	2.8 ± 0.3	NS
LVEDD, mm	13.2 ± 0.5	17.1 ± 0.7	<0.05	13.7 ± 0.4	16.5 ± 0.3	<0.05
LVESD, mm	7.9 ± 0.4	14.4 ± 0.6	<0.01	8.4 ± 0.3	14.0 ± 0.5	<0.01
FS, %	39.7 ± 1.6	15.3 ± 1	<0.001	38.0 ± 1.6	15.0 ± 1.5	<0.001
LVEDP, mmHg	3.5 ± 0.4	14.3 ± 1.2	<0.001	2.9 ± 0.3	14.0 ± 1.0	<0.001
LVSP, mmHg	90.0 ± 7.0	67.0 ± 8.0	<0.01	82.0 ± 9.0	68.0 ± 6.0	<0.01
LV +*dp/dt*, mmHg/sec	1557 ± 104	896 ± 68	<0.005	1502 ± 101	883 ± 150	<0.005

[a]Values represent means ± SEM. HR, heart rate (beats/min [bpm]); LVEDD, left ventricular (LV) end-diastolic dimension; LVESD, LV end-systolic dimension; FS, fractional shortening calculated as % FS = [(EDD − ESD)/EDD] × 100; LVEDP, LV end-diastolic pressure; LVSP, LV end-systolic pressure; dp/dt_{max}, maximum rate of LV pressure development.

increase in left ventricular (LV) end-diastolic dimension and a reduction of fractional shortening (FS) in the CHF rabbits (Table 1). *In vivo* hemodynamic measurements demonstrated higher left ventricular end-diastolic pressure and lower LV contractility (assessed by LV $+dp/dt$) in the paced animals. LV dimensions, calculated FS, basal hemodynamics, and LV $+dp/dt$ were unaffected by adenoviral gene transfer (Table 1).

Apoptotic parameters in failing myocardium

To assess biochemical hallmarks of apoptosis in the hearts of paced rabbits, a series of molecular analyses was performed. In cytosolic cell extracts prepared from failing and sham-operated LV myocardium, a significant (~6-fold) increase in caspase 3 activity was documented in the CHF tissue after 15 days of pacing (84 ± 5.3 vs. 15.8 ± 3.1 active units; sham, $n = 6$; CHF 7 days, $n = 4$; CHF 15 days, $n = 8$; Fig. 1A). To examine the ability of cell lysates of failing myocardium to cause DNA degradation *in vitro*, liver nuclei were incubated with extracts of CHF heart tissue and DNA was analyzed by agarose gel electrophoresis (Enari *et al.*, 1995). DNA fragmentation activity, producing the typical DNA ladder showing multiples of 180 bp, was already present after 7 days of pacing in failing myocardium but not in tissue of sham-operated animals ($n = 4$ in each group; Fig. 1B). The nuclease responsible for DNA degradation in the caspase 3 apoptotic pathway is CAD, which is produced as a complex with its inhibitor ICAD (Enari *et al.*, 1998). We used immunoblotting of cytosolic fractions from failing myocytes to assess the evidence of ICAD cleavage. The ICAD subunit of ~45 kDa was relatively stable in sham-operated control myocardium. In contrast, a main 12-kDa cleavage product was present in failing tissue and in lysates of healthy myocardium after incubation with recombinant caspase 3. This cleavage of ICAD was blocked in the presence of the caspase 3 inhibitor DEVD-FMK ($n = 6$ in each group; Fig. 1C).

In end-stage heart failure, apoptosis is accompanied by DNA degradation (Olivetti *et al.*, 1997). The number of apoptotic nuclei was evaluated in sham-operated and failing myocardium by terminal deoxynucleotidyltransferase (TdT)-mediated dUTP nick end labeling (TUNEL) staining ($n = 3$ in each group; Fig. 2A). Simultaneous α-sarcomeric actin staining confirmed that apoptotic nuclei were predominantly in cardiomyocytes. The increase in TUNEL-positive myocytes assessed by semiquantitative scoring correlated with DNA–histone formation in failing myocardium (Fig. 2B and C). As shown in Fig. 2C, whole cell extracts from myocardium after 15 days of pacing had an almost 6-fold increase in histone-associated DNA fragments compared with extracts from sham-operated controls (sham, $n = 6$; CHF 7 days, $n = 4$; CHF 15 days, $n = 8$). The apoptotic changes regarding caspase 3 and CAD activities, TUNEL-positive nuclei, and nuclear DNA fragmentation consistently increased with the duration of pacing in this animal model (Fig. 1A and B; Fig. 2B and C).

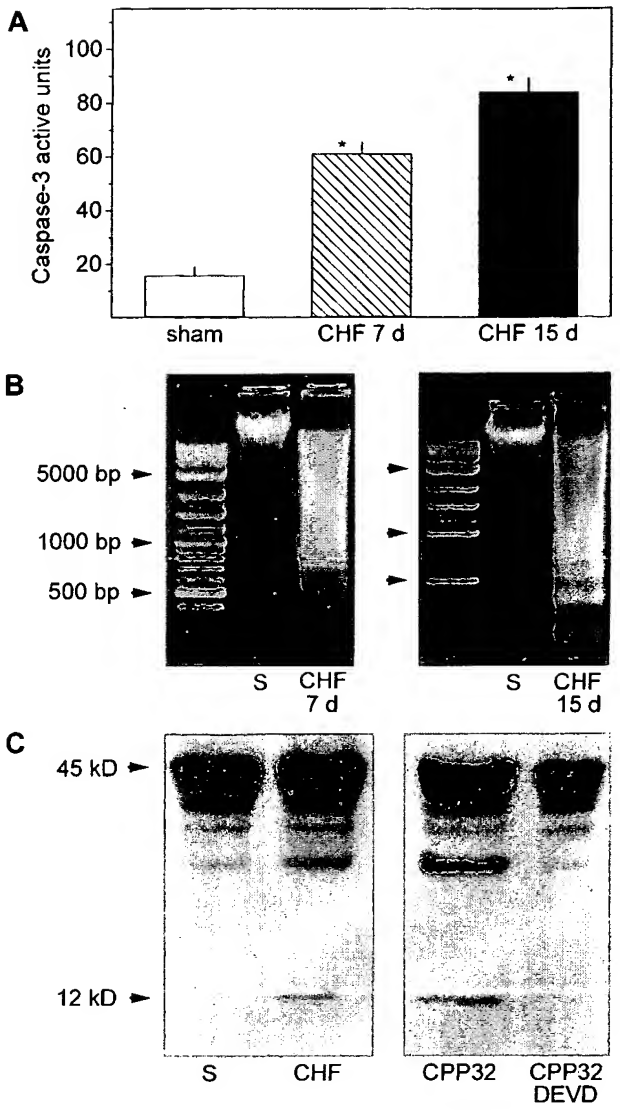

FIG. 1. Induction of caspase 3-mediated CAD activation in myocardium of sham-operated (sham) or paced (CHF) animals. (**A**) Caspase 3 enzyme activity levels measured in cytosolic fractions of anterolateral LV tissue. Data are expressed as means ± SEM. Sham, $n = 6$; CHF 7 days, $n = 4$; CHF 15 days, $n = 8$. $^*p < 0.005$ in comparison with sham. (**B**) Fragmentation of genomic DNA purified from isolated rat liver nuclei incubated with cytosolic extracts of sham-operated (S) and failing heart after 7 days (CHF 7 d) and 15 days (CHF 15 d) of pacing. Shown are representative data from one of four animals in each group. (**C**) Immunoblot analysis of native ICAD cleavage in lysates of myocardium from sham-operated (S) and failing rabbits (CHF). Tissue samples from sham-operated controls were incubated with recombinant human caspase 3 (CPP32) and its tetrapeptide inhibitor DEVD-FMK (CPP32 DEVD). Shown are representative results from one of six animals in each group.

Transcoronary gene delivery and time course of transgene expression

To manipulate caspase 3-activated apoptosis, an adenoviral construct for p35 as a potent caspase inhibitor was generated. Adenovirus was structured to encode transgene and GFP as reporter gene. In addition, the transgene was epitope tagged for immunostaining. We have previously demonstrated robust expression of adenoviral transgenes in rabbit myocardium by *in vivo* transcoronary delivery in the left coronary system after serotonin and low calcium pretreatment (Weig *et al.*, 2000).

Fluorescence imaging of microscopic sections of sham-operated heart infected with bicistronic Ad-p35 revealed high levels of GFP expression throughout the manipulated myocardium.

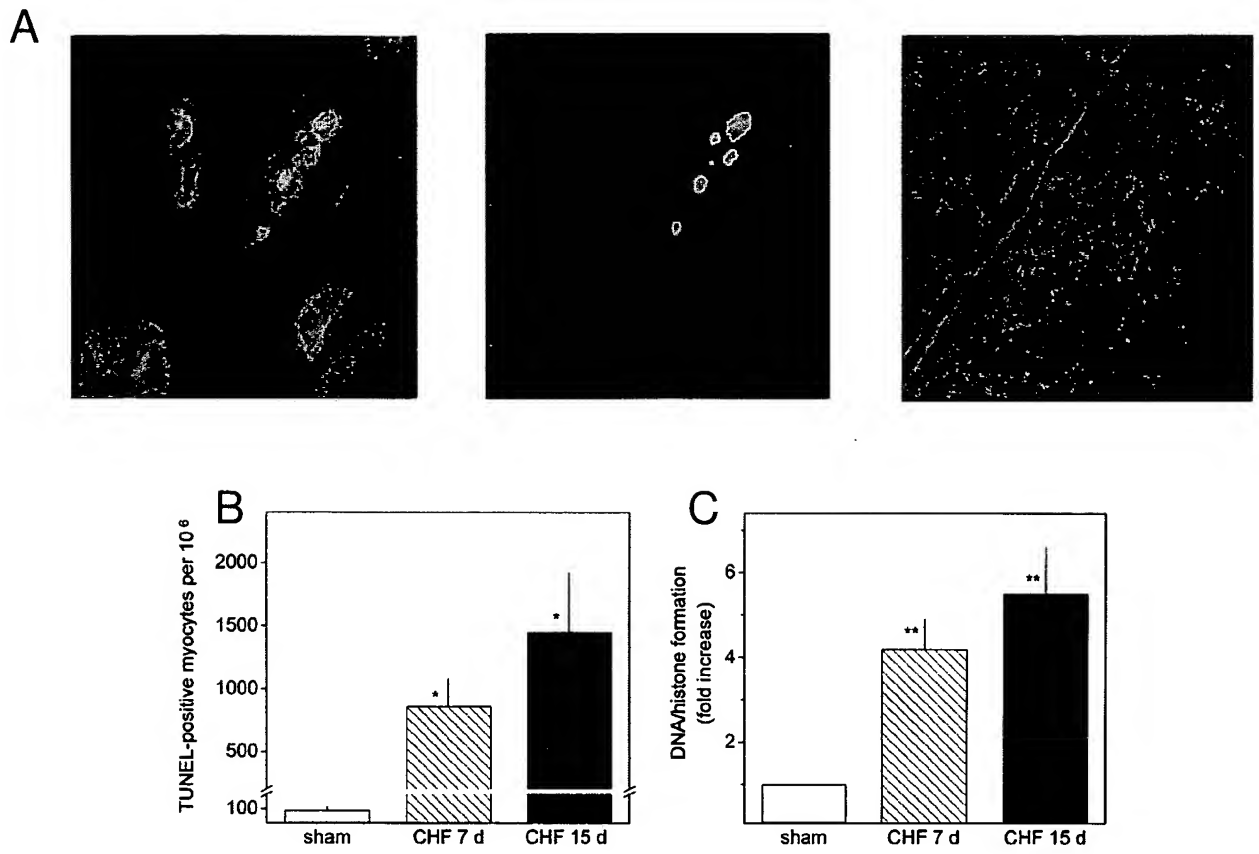

FIG. 2. Nuclear apoptosis in paced myocardium. (**A**) Fluorescence imaging of heart sections (7 μm) after 15 days of rapid ventricular pacing. Blue fluorescence (420 nm) illustrates nuclei by Hoechst 33258 and green fluorescence (520 nm) shows apoptotic nuclei identified by TUNEL staining. Immunostaining for α-sarcomeric actin reflects myocytes (red fluorescence, 615 nm). Original magnification: ×630. Shown are representative sections from one of three hearts. (**B**) Semiquantitative analysis of myocyte apoptosis detected by TUNEL staining in sham-operated (sham) and failing hearts after 7 days (CHF 7 d) and 15 days (CHF 15 d) ventricular pacing. Data are expressed as means ± SEM; $n = 3$ animals in each group. $*p < 0.01$ in comparison with sham. (**C**) DNA–histone complex formation measured in cytosolic fractions of anterolateral LV tissue. Data are expressed as means ± SEM. Sham, $n = 6$; CHF 7 days, $n = 4$; CHF 15 days, $n = 8$. $**p < 0.005$ in comparison with sham.

Immunostaining for the epitope-tagged transgene showed signals in the same area restricted to the anterolateral wall, corresponding to the perfusion bed of the circumflex artery, the dominant left coronary artery in rabbits (Fig. 3A). To quantify gene expression after transcoronary delivery, we isolated single cardiomyocytes from LV myocardium of sham-operated and GFP-infected rabbits and performed flow cytometry studies for GFP fluorescence 0, 4, 7, and 15 days after infection. In comparison with background fluorescence on day 0, GFP expression clearly increased at 4 days (44%) and 7 days (37%), but gradually declined after 15 days (26%) (Fig. 3B). These data are in accordance with other first-generation adenoviral gene transfer studies (Donahue *et al.*, 2000). We did not observe any GFP expression differences between failing or nonfailing tissue.

No evidence of cell necrosis was present in samples from LV myocardium of 15-day paced animals that had received gene transfer of Ad-p35 and Ad-GFP ($n = 6$). Fifteen days after gene delivery, we observed a mild inflammatory infiltration, mainly of mononuclear cells, both in Ad-p35- and Ad-GFP-infected myocardial tissue.

p35 expression blocks caspase 3 activity and DNA fragmentation in vitro and in failing myocardium in vivo

Before determining the functional consequences of adenoviral infection in failing myocardium, we examined the expression and function of p35 in TNF-α-stimulated apoptotic ventricular myocytes in culture (Fig. 4A and B). TNF-α is an autocrine contributor to myocardial dysfunction and an inductor of programmed cell death in several cardiac diseases (Krown *et al.*, 1996). Because rabbit TNF-α is not available, we performed *in vitro* experiments in adult cardiomyocytes isolated from rat hearts. Forty-eight hours after Ad-p35 infection *in vitro*, extracts from rat myocytes expressed significant levels of recombinant protein, as determined by immunoblotting (data not shown). In TNF-α-treated cells, caspase 3 activity and nucleosome formation were significantly increased. Adenoviral expression of p35 efficiently suppressed TNF-α-stimulated caspase 3 activity to basal levels ($n = 4$ animals; Fig. 4A and B).

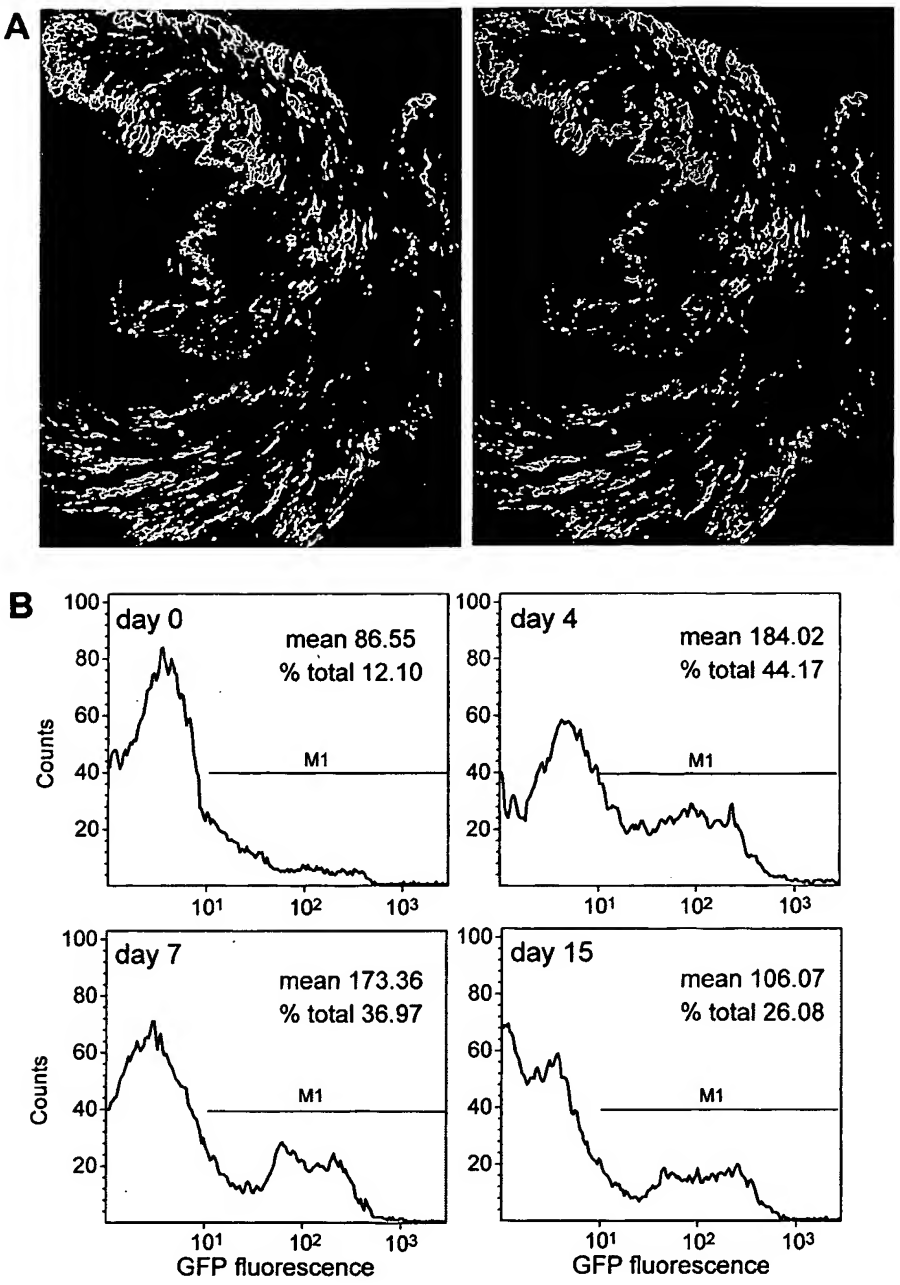

FIG. 3. Transgene expression in LV myocardium after *in vivo* transcoronary adenovirus application. (**A**) Microscopic slices (3 μm) of sham-operated rabbit heart 4 days after infection with bicistronic adenovirus coding for GFP and p35 (5×10^{10} PFU). Direct p35 expression was documented by immunostaining with a monoclonal anti-FLAG M2 antibody directed against the artificial epitope. The samples were visualized by phase-contrast fluorescence microscopy at 520 nm for GFP (*left*) and at 615 nm (Texas Red fluorescence) for p35 (*right*). Original magnification: ×25. (**B**) Time course of GFP expression was analyzed by flow cytometry experiments in freshly isolated cardiomyocytes from sham-operated rabbit myocardium after Ad-GFP gene delivery. M1 indicates the GFP fluorescence cutoff; 2×10^4 cells were analyzed in each sample. Shown are cumulative data from four animals (one animal each day).

Next, we serially examined *in vivo* expression of p35 4, 7, and 15 days after adenoviral gene transfer in sham-operated animals by immunoblotting. p35 expression showed a maximum after 4–7 days and gradually decreased at day 15 (Fig. 4C). Cell extracts prepared from failing myocardium after 15 days of pacing documented a significant increase in caspase 3 activity, and a 5.5-fold caspase 3-mediated induction of DNA fragmentation compared with sham-operated controls (Fig. 4D and E). Gene delivery of Ad-p35 to failing hearts efficiently blocked caspase 3 stimulation (28 ± 11 vs. 84 ± 5.3 active units) and clearly reduced DNA–histone formation in comparison with CHF (2.7- vs. 5.5-fold increase; sham, $n = 6$; CHF, $n = 8$; CHF+Ad-p35, $n = 4$; CHF+Ad-GFP, $n = 4$; Fig. 4D and E).

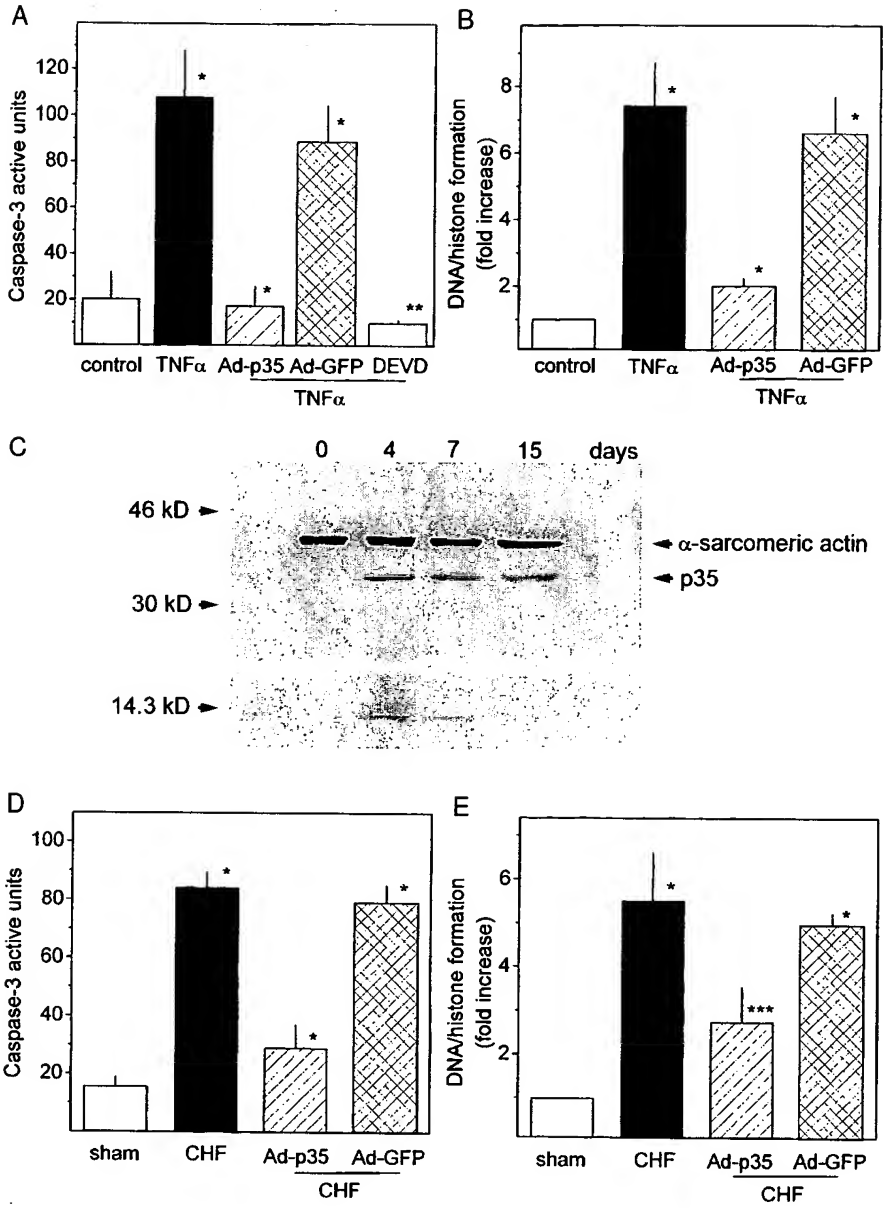

FIG. 4. Blockade of caspase 3 activity and nucleosome formation by adenoviral overexpression of p35 *in vitro* and *in vivo*. (**A**) Caspase 3 activity and (**B**) DNA–histone formation determined in lysates of isolated rat cardiomyocytes infected *in vitro* with Ad-p35 and Ad-GFP (MOI of 100 PFU/cell). Apoptosis was induced in the infected cells by incubation with rat TNF-α (3500 IU/ml) for 18 hr. The tetrapeptide inhibitor of caspase 3 (DEVD-FMK) was applied in a concentration of 5 μM. Data in (**A**) and (**B**) are expressed as means ± SEM; $n = 4$ per each group. (**C**) Immunoblot analysis of extracts from anterolateral wall of Ad-p35-infected rabbit myocardium 0, 4, 7, and 15 days after gene transfer. Immunostaining was performed with two monoclonal antibodies, anti-FLAG M2 and anti-α-sarcomeric actin, to document in parallel p35 and actin expression. Shown are cumulative data from four animals (one animal each day). (**D**) Caspase 3 enzyme activity levels and (**E**) DNA–histone formation assessed in ventricular tissue from sham-operated (sham) and failing hearts (CHF). Rabbits were paced for 15 days and received an intracoronary application of Krebs-Ringer, Ad-p35, or Ad-GFP. Data in (**D**) and (**E**) are expressed as means ± SEM. Sham, $n = 6$; CHF, $n = 8$; CHF+Ad-p35, $n = 4$; CHF+Ad-GFP, $n = 4$. $^*p < 0.005$, $^{**}p < 0.001$, and $^{***}p < 0.01$ in comparison with control/sham or TNF-α-stimulated/CHF cardiomyocytes.

Blocking caspase 3 activation improves contractile force in vivo

To assess the functional effects of p35 in preventing the progression of heart failure as cytosolic modulator of myocardial programmed cell death, we measured echocardiographic and hemodynamic parameters after adenovirus-mediated gene delivery. FS was measured after 7 and 15 days of pacing in CHF rabbits and failing animals that received Ad-p35 or Ad-GFP (Fig. 5A and B). FS was significantly elevated at day 15 after

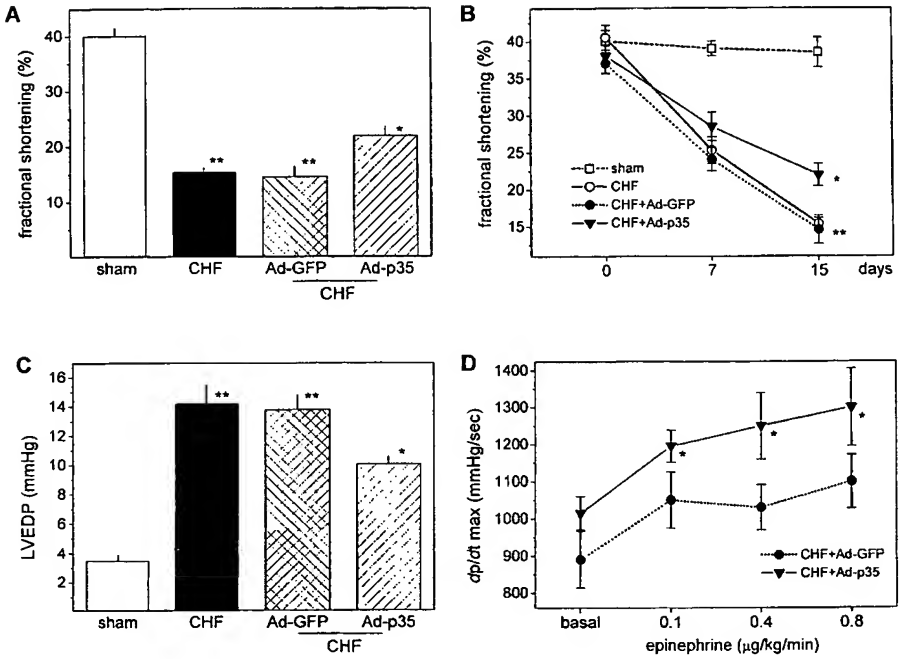

FIG. 5. Echocardiographic and hemodynamic measurements in genetically manipulated hearts infected with Ad-p35. (**A**) FS and (**C**) LVEDP were assessed in sham-operated (sham) and failing hearts (CHF) after 15 days of pacing and transcoronary application of Krebs-Ringer, Ad-GFP, or Ad-p35. (**B**) Time course of fractional shortening after 7 and 15 days of pacing. (**D**) dp/dt_{max} recordings after administration of increasing doses of epinephrine. Data are shown as means ± SEM, $n = 8$ per each group. $^*p < 0.05$, $^{**}p < 0.001$ in comparison with sham and CHF+Ad-GFP hearts.

rapid ventricular pacing in CHF+Ad-p35 animals, whereas no effect was seen in CHF+Ad-GFP rabbits (22 ± 1 vs. 15.0 ± 1.5%, $n = 8$ in each group, $p < 0.05$).

Left ventricular end-diastolic pressure (LVEDP) and $+dp/dt$ as characteristics of global ventricular contractility were determined to complement the echocardiographic information. LVEDP in CHF+Ad-p35 animals was reduced compared with the CHF+Ad-GFP group (10.4 ± 0.8 vs. 14.0 ± 1 mmHg, $n = 8$ in each group, $p < 0.05$; Fig. 5C). When cytosolic caspase activity was blocked by overexpression of p35 up to 15 days over the pacing period, cardiac contractility in rabbits, as measured by LV $+dp/dt$, was significantly enhanced in response to epinephrine compared with Ad-GFP-treated failing hearts (Fig. 5D).

The failing hearts in this model had no significant increase in LV mass when normalized to either tibial length or body weight. Overexpression of p35 in the paced hearts did not have any significant effect on LV mass, normalized to tibial length or body mass (Table 2).

Functional reconstitution of contractile force by overexpression of p35 by reducing sarcomeric disarray

To investigate the effect of p35 expression on contractile function of single ventricular cardiomyocytes 15 days after *in vivo* gene delivery, cells from the target area of sham+Ad-GFP, CHF+Ad-GFP, and CHF+Ad-p35 myocardium were isolated. Transgene-expressing cells were selected by GFP fluorescence. Figure 6A–C show confocal laser scanning microscopy of isolated myocytes after phalloidin staining to visualize polymeric actin. Interestingly, failing cardiomyocytes expressing p35 showed a better organized sarcomeric structure compared with

TABLE 2. MORPHOMETRIC ANALYSES[a]

Group ($n = 4$)	*Body weight* (*g*)	*LV weight* (*g*)	*LV/BW* ($\times 10^3$)	*LV/TL* ($\times 10^3$) (*g/cm*)
Sham + Ad-GFP	2900 ± 305	9.7 ± 0.6	3.28 ± 0.8	950 ± 59
CHF + Ad-GFP	2800 ± 346	9.4 ± 0.8	3.32 ± 0.4	921 ± 37
Sham + Ad-p35	2950 ± 423	9.5 ± 0.4	3.20 ± 0.9	931 ± 45
CHF + Ad-p35	2740 ± 502	9.8 ± 0.9	3.51 ± 0.7	960 ± 74

Abbreviations: LV, left ventricle; BW, body weight; TL, tibial length.
[a]For all groups no significant values were reached.

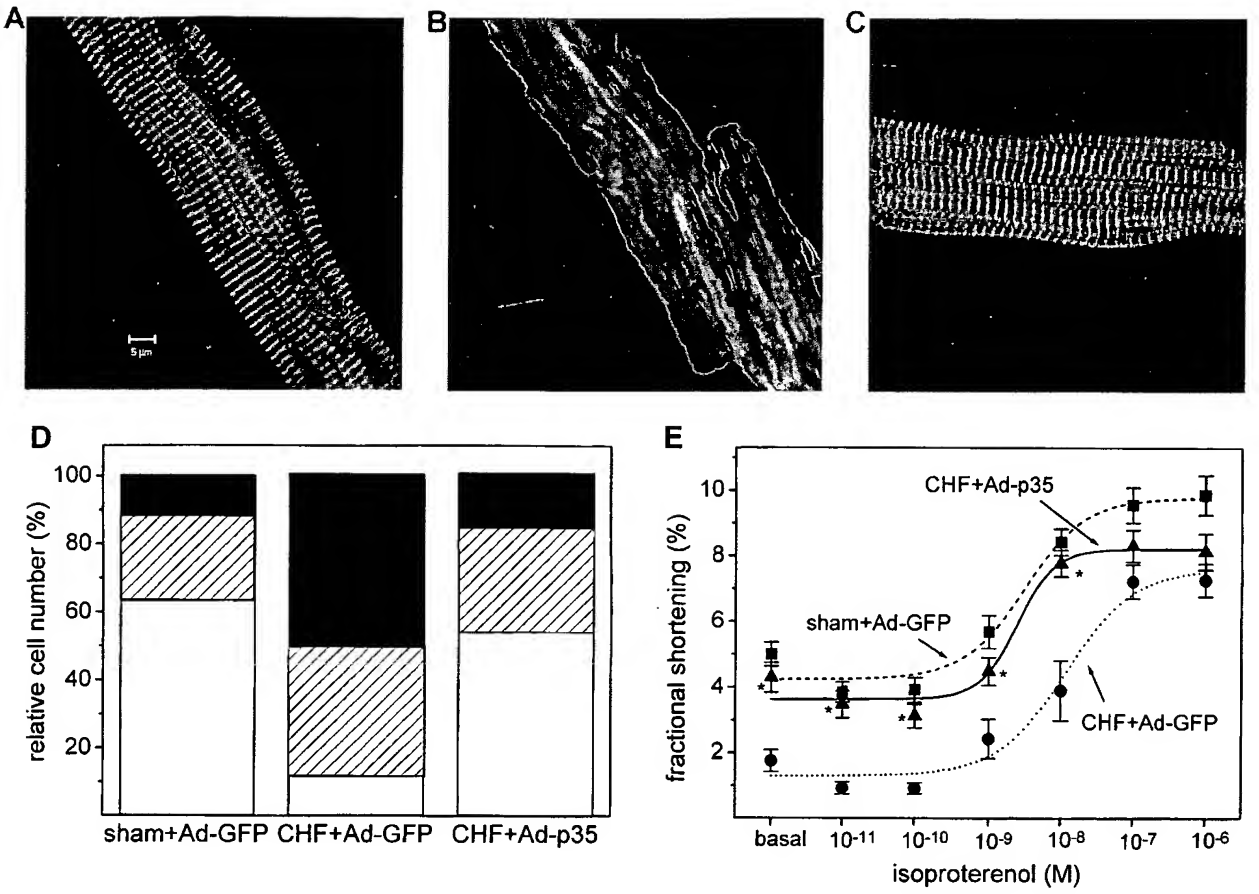

FIG. 6. Effect of p35 expression on sarcomere organization and contractile performance of myocytes from paced hearts. Ventricular rabbit cardiomyocytes were isolated from the anterolateral wall of sham-operated Ad-GFP-infected (**A**), failing Ad-GFP-infected (**B**), and failing Ad-p35-infected myocardium (**C**) and visualized by laser scanning fluorescence microscopy after phalloidin staining. Scale bar corresponds to 5 μm. (**D**) Morphology of phalloidin-stained myofibrils was semiquantitatively scored on the basis of the area occupied by organized sarcomere in total cell area: poor, less than one-third (black pattern); moderate, less than two-thirds (striped pattern); good, more than two-thirds (white pattern). Eight hundred cells isolated from 4 animals were counted for each group. (**E**) Contraction amplitude in isolated cardiomyocytes after *in vivo* gene delivery of Ad-p35 and Ad-GFP in sham-operated or paced rabbits. Data in (**E**) are expressed as means ± SEM, $n = 60$ cells from four rabbits in each group. $^*p < 0.001$ in comparison with CHF+Ad-GFP.

Ad-GFP-infected failing cells with destroyed sarcomeric units. The degree of sarcomere organization assessed by semiquantitative scoring of rod-shaped cells is presented in Fig. 6D. The ratio of myocytes with well-organized sarcomeres (more than two-thirds of cell area) was 64 ± 1% in sham+Ad-GFP, 13 ± 3% in CHF+Ad-GFP, and 52 ± 4% in CHF+Ad-p35 cardiomyocytes (800 rod-shaped cells, expressing the transgene, and isolated from four animals were analyzed in each group). The percentage of round, dead cells was 28 ± 4%, 39 ± 8%, and 20 ± 6%, respectively (2000 cells isolated from 4 animals were randomly selected and counted in each group).

Shortening amplitude was measured in failing and nonfailing cells from myocardium infected *in vivo* with Ad-p35 or Ad-GFP, electrically stimulated at a rate of ~70 contractions per minute. Experiments were performed in myocytes with moderate or good sarcomeric structure. Adenoviral infection did not alter shortening characteristics. As shown in Fig. 6E, failing cardiomyocytes expressing p35 presented a significantly increased basal shortening amplitude compared with equivalent myocytes infected with Ad-GFP (4.3 ± 0.4 vs. 1.8 ± 0.2%, $n = 60$ in each group, $p < 0.001$). This enhancement of contractile force was also seen after isoproterenol stimulation and the EC_{50} of the dose–response curve was shifted to higher values, similar to those of nonfailing cells treated with Ad-GFP (Fig. 6E). These results indicate that p35 restores sarcomeric organization and thereby reconstitutes contractile performance of failing myocytes.

Microinjection of activated caspase 3 in isolated ventricular cardiomyocytes

To examine whether activation of caspase 3 is sufficient for induction of sarcomeric disarray, we microinjected activated enzyme into the cytoplasm of rabbit ventricular healthy cardiomyocytes. Positive cells (~10–20%) were identified by FITC fluorescence. Morphological characteristics of cardiomyocytes 2 hr after microinjection of activated caspase 3 (4 and 20 ng/μl) compared with control-injected cells are presented in

Fig. 7A and B. Treatment of myocytes with caspase 3 caused a rapid, concentration-dependent destruction of the straight and striated bundles of the sarcomeric units (Fig. 7B, left and right). Single-cell shortening experiments in microinjected cardiomyocytes showed a caspase 3-mediated reduction in basal and isoproterenol-stimulated contraction (4.3 vs. 9.8% [10^{-8} *M* isoproterenol], $n = 45$ in each group, $p < 0.005$). These effects were blocked by preincubation of the myocytes with DEVD-FMK (Fig. 7C).

DISCUSSION

In the present study, we report the novel finding that caspase activation influences cardiac performance of failing ventricular myocytes by destroying sarcomeric structure. Caspase 3 activation, present in failing myocardium, can be corrected via adenovirus-mediated gene delivery of p35 with a positive impact on contractility.

In at least four different models of ischemia–reperfusion injury (cardiac, renal, cerebral, and liver), caspase inhibition has resulted in decreased infarct volumes and partially improved organ function (Nicholson, 2000). However, no information was previously available as to whether caspase activation contributes to disease progression in heart failure and whether cardiomyocytes rescued from apoptosis under such conditions preserve their contractile function. Caspases have multiple intracellular targets involved in chromatin condensation, DNA fragmentation, and cytoskeletal destruction (Hengartner, 2000). In cardiac myocytes, the cytoskeleton is a highly specialized structure, whose components can be classified into three groups: (1) the force-generating contractile sarcomeric unit (e.g., actin–myosin filaments, troponin–tropomyosin complex), (2) the intrasarcomeric cytoskeleton regulating the contraction cycle (e.g., titin, α-actinin, and myosin-binding protein C), and (3) the extrasarcomeric cytoskeleton (e.g., desmin, lamins, and dystrophin) (Chen and Chien, 1999). The impact of abnormalities in the cytoskeleton–sarcomeric network on cardiac function has been demonstrated in hereditary forms of hypertrophic and dilated cardiomyopathy (Towbin, 1998; Kamisago *et al.*, 2000). In addition, cleavage of dystrophin by enteroviral protease 2A has been suggested as a molecular mechanism for acquired forms of dilated cardiomyopathy (Badorff *et al.*, 1999). These findings indicate that defective transmission of force through loss of sarcomere integrity or cytoskeletal structures leads to myocyte dysfunction.

In a rabbit model of CHF, we investigated whether activation of caspases contributes to disease progression and influences contractility by sarcomere disorganization. Pacing-induced heart failure has served as a useful experimental model for the study of dilated cardiomyopathy, which is associated with enhanced expression of *bax*, a gene that stimulates apoptosis (Leri *et al.*, 1998). To manipulate caspase activation in failing myocardium, we used the baculoviral cell survival protein p35, which blocks apoptosis induced by TNF, Fas, glucocorticoids, radiation, and DNA-damaging agents by inhibiting caspases 1, 2, 3, 4, 6, 7, 8, and 10 (Villa *et al.*, 1997).

Four lines of evidence support the notion that caspases play a role in the development of CHF. First, the activities of caspase 3 and CAD, two key molecules in the process of myocardial apoptosis, are increased in this CHF model (Fig. 1). Similar findings for caspase 3 in biopsies of human cardiomyopathic hearts confirm our results (Narula *et al.*, 1999). Second, somatic gene delivery of p35 into failing myocardium significantly reduced caspase 3 activity and nucleosome formation *in vivo* (Fig. 4). Echocardiographic and hemodynamic function of the p35-expressing hearts was partially restored (Fig. 5).

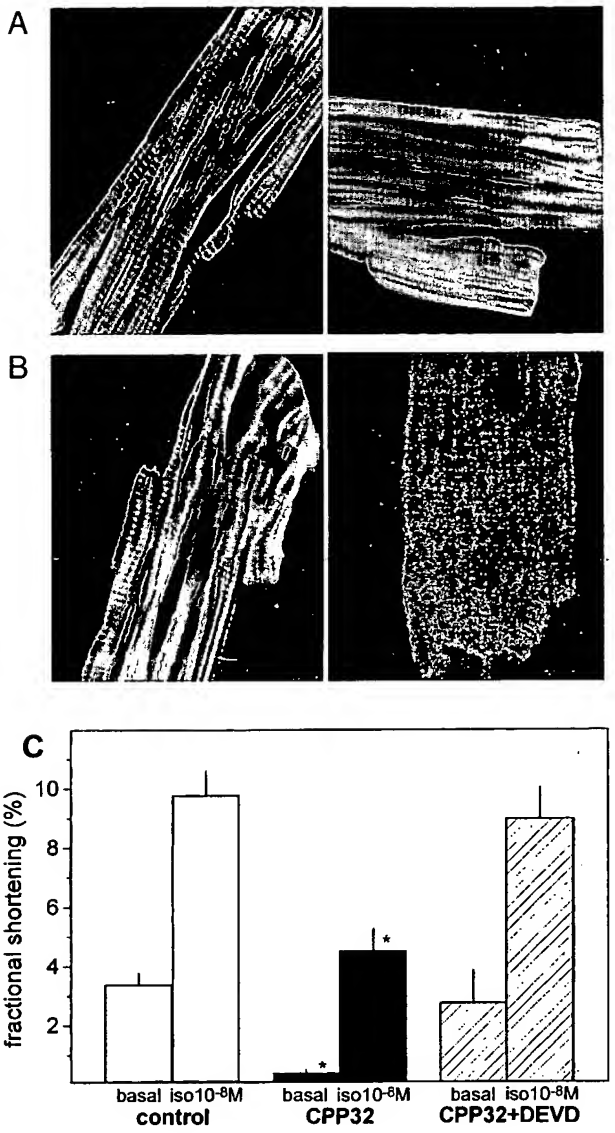

FIG. 7. Microinjection of activated caspase 3 into the cytoplasm of healthy ventricular cardiomyocytes. (**A**) Myocytes were microinjected with FITC-conjugated dextran alone or (**B**) plus human recombinant active caspase 3 (4 ng/μl, *left*; 20 ng/μl, *right*). The morphology of actin fibers was visualized by laser scanning fluorescence microscopy after phalloidin staining. Original magnification: ×630. (**C**) Contraction amplitude under basal conditions and isoproterenol stimulation (10^{-8} *M*) was determined in cells 2 hr after microinjection of FITC-conjugated dextran (open columns) or caspase 3 at 4 ng/μl (CPP32) (solid columns). Preincubation of DEVD-FMK was performed (hatched columns). Data are shown as means ± SEM, $n = 45$ cells from two animals in each group. *$p < 0.005$ in comparison with control injected cells (basal; isoproterenol 10^{-8} *M*).

These results are in accordance with previously published data about reconstitution of visual function in a retinitis pigmentosa model in *Drosophila* by caspase 3 inhibition (Davidson and Steller, 1998). Third, isolated cardiomyocytes of failing hearts treated with Ad-p35 showed significantly increased basal and isoproterenol-stimulated fractional shortening and better organized sarcomeric structure (Fig. 6). Because p35 expression had no positive inotropic effect in healthy cardiomyocytes *in vitro* (data not shown), one might speculate that its preservation of contractile force is due to irreversible caspase inhibition. Fourth, cytoplasmic microinjection of activated caspase 3 in healthy cells induced a concentration-dependent destruction of the sarcomeric units, as demonstrated by phalloidin staining of polymerized actin, and correlated with reduced contractile performance (Fig. 7).

Several mechanisms may cause caspase-mediated sarcomere disorganization in failing cardiomyocytes. Caspase 3-mediated activation of gelsolin and a consecutive shift of polymerized actin to monomeric actin in the sarcomeric unit can be discussed as one molecular mechanism (Sun *et al.*, 1999). Another possibility for caspase-induced sarcomere destruction is the direct cleavage of actin by caspase 3, because cytoskeletal actin is a substrate of caspases (Mashima *et al.*, 1999). Further studies should investigate the interaction of caspase 3 with other sarcomere proteins, because putative cleavage sites are located in the ATP-binding domain of the myosin heavy chain, in troponin T and I, tropomyosin, and tropomodulin. Another important issue to be elucidated is whether myocytes with poor organized sarcomere show caspase 3 activation without nuclear DNA damage in order to examine whether caspases play a role in the deterioration of cell function in the absence of triggering the full death program.

Cardiac-specific deletion of the signaling receptor subunit, gp130, leads to massive cardiac apoptosis and accelerated dilated cardiomyopathy after aortic banding (Hirota *et al.*, 1999). Further investigations should determine the existence of an intersection between the proapoptotic caspase 3 pathway and the antiapoptotic gp130 survival pathway in CHF.

Limitations of this study are (1) transcoronary gene delivery, which affects only a limited area of LV myocardium, and (2) the use of first-generation adenoviral vectors, which induce an inflammatory response and result in transient gene expression. In rabbits, the left coronary system is dominant and the circumflex artery is by far the largest coronary vessel. The gene delivery protocol via the left coronary system used in this study affected ~30% of the whole LV myocardium 4 days after *in vivo* infection (Fig. 3). Hajjar *et al.* established a catheter-based technique that allows for generalized cardiac gene transfer *in vivo* (Hajjar *et al.*, 1998). However, our group and Lai *et al.* reported functional modulation of cardiac performance *in vivo* by using intracoronary adenovirus delivery after modification of the endothelial barrier (Lai *et al.*, 2000; Weig *et al.*, 2000). Infection of rabbit myocardium with recombinant adenoviruses did not affect myocyte apoptosis, as had already been observed *in vitro* (Matsui *et al.*, 1999). Histologic slices showed a mild inflammatory infiltrate 15 days after gene transfer, equally in the Ad-p35- and Ad-GFP-treated group. Therefore, we believe the immunological response did not confound our results.

Fifteen days after gene transfer, ~14% of the cardiomyocytes from whole LV myocardium showed GFP fluorescence. By using a bicistronic vector to control transgene expression and by studying functionally isolated myocytes from the target area, we were able to verify that the observed increase in contractility *in vivo* was directly mediated by caspase inhibition in cardiomyocytes.

Because the molecular mechanism of p35 is not a direct cAMP- or Ca^{2+}-regulated positive inotropism, but a protection from sarcomere disorganization via irreversible caspase inhibition, protein synthesis is necessary to counteract its effect (Bump *et al.*, 1995). Although p35 expression and caspase 3 activity were inversely correlated over the time course of heart failure development, transgene levels documented in the first week of pacing should be sufficient to block tachycardia-induced caspase activation, and thereby delay heart failure in this animal model.

In summary, we have ameliorated systolic function in failing myocardium by blocking caspases through gene transfer of recombinant adenovirus expressing p35. Improved contractile function and reduced LV end-diastolic pressures were associated with reduction in caspase 3 activity, DNA fragmentation, and sarcomere disorganization. This study provides evidence that caspase activation contributes to the progression of heart failure and that its prevention leads to partial restoration of cardiac hemodynamics.

NOTE ADDED IN PROOF

During the review process of the present article, myocyte apoptosis assessed by caspase 3 and CAD activities and TUNEL staining has been reported in a similar model of rapid ventricular pacing in dogs by Cesselli *et al.* (Circ. Res. 2001;89:279–286).

ACKNOWLEDGMENTS

We thank Dr. S. Nagata (Department of Genetics, Osaka University Medical School, Japan) and Dr. H. Steller (Howard Hughes Medical Research Institute, MIT) for helpful discussions and for providing us with the p35 cDNA.

These studies were supported by the Deutsche Forschungsgemeinschaft and Bayerische Forschungsmittel der Technischen Universität München.

REFERENCES

AKHTER, S., SKAER, C., KYPSON, A.P., McDONALD, P.H., PEPPEL, K., GLOWER, D., LEFKOWITZ, R.J., and KOCH, W.J. (1997). Restoration of β-adrenergic signaling in failing cardiac ventricular myocytes via adenoviral-mediated gene transfer. Proc. Natl. Acad. Sci. U.S.A. **94,** 12100–12105.

ASHKENAZI, A., and DIXIT, V.M. (1998). Death receptors: Signaling and modulation. Science **281,** 1305–1308.

BADORFF, C., LEE, G.H., LAMPHEAR, B.J., MARTONE, M.E., CAMPBELL, K.P., RHOADS, R.E., and KNOWLTON, K.U. (1999). Enteroviral protease 2A cleaves dystrophin: Evidence of cytoskeletal disruption in an acquired cardiomyopathy. Nat. Med. **5,** 320–326.

BRAUNWALD, E., and BRISTOW, M.R. (2000). Congestive heart failure: Fifty years of progress. Circulation **102,** IV14–IV23.

BUMP, N.J., HACKETT, M., HUGUNIN, M., SOMASEKAR, S., BRADY, K., CHEN, P., FERENZ, C., FRANKLIN, S., GHAYUR, T., LI, P., LICARI, P., MANKOVICH, J., SHI, L., GREENBERG,

A.H., MILLER, L.K., and WONG, W.W. (1995). Inhibition of ICE family proteases by baculovirus antiapoptotic protein p35. Science **269,** 1885–1888.

CHEN, J., and CHIEN, K.R. (1999). Complexity and simplicity: Monogenic disorders and complex cardiomyopathies. J. Clin. Invest. **103,** 1483–1485.

DAVIDSON, F.F., and STELLER, H. (1998). Blocking apoptosis prevents blindness in *Drosophila* retinal degeneration mutants. Nature **391,** 587–591.

DONAHUE, J.K., HELDMAN, A.W., FRASER, H., McDONALD, A.D., MILLER, J.M., RADE, J.J., ESCHENHAGEN, T., and MARBAN, E. (2000). Focal modification of electrical conduction in the heart by viral gene transfer. Nat. Med. **6,** 1395–1398.

ENARI, M., HASE, A., and NAGATA, S. (1995). Apoptosis by a cytosolic extract from Fas-activated cells. EMBO J. **14,** 5201–5208.

ENARI, M., SAKAHIRA, H., YOKOYAMA, H., OKAWA, K., IWAMATSU, A., and NAGATA, S.A. (1998). Caspase-activated DNase that degrades DNA during apoptosis, and its inhibitor ICAD. Nature **391,** 43–50.

GARDIN, J.M., SIRI, F.M., KITSIS, R.N., EDWARDS, J., and LEINWAND, L.A. (1995). Echocardiographic assessment of left ventricular mass and systolic function in mice. Circ. Res. **76,** 907–914.

GREEN, D.R., and REED, J.C. (1998). Mitochondria and apoptosis. Science **281,** 1309–1312.

HAJJAR, R.J., SCHMIDT, U., MATSUI, T., GUERRERO, L., LEE, K.H., GWATHMEY, J., DEC, W., SEMIGRAN, M.J., and ROSENZWEIG, A. (1998). Modulation of ventricular function through gene transfer *in vivo*. Proc. Natl. Acad. Sci. U.S.A. **95,** 5251–5256.

HAUNSTETTER, A., and IZUMO, S. (2000). Toward antiapoptosis as a new treatment modality. Circ. Res. **86,** 371–376.

HE, T.C., ZHOU, S., DA COSTA, L.T., YU, J., KINZLER, K.W., and VOGELSTEIN, B. (1998). A simplified system for generating recombinant adenoviruses. Proc. Natl. Acad. Sci. U.S.A. **95,** 2509–2514.

HENGARTNER, M.O. (2000). The biochemistry of apoptosis. Nature **407,** 770–776.

HIROTA, H., CHEN, J., BETZ, U.A., RAJEWSKY, K., GU, Y., ROSS, J., MULLER, W., and CHIEN, K.R. (1999). Loss of a gp130 cardiac muscle cell survival pathway is a critical event in the onset of heart failure during biomechanical stress. Cell **97,** 189–198.

HUNTER, J.J., and CHIEN, K.R. (1999). Mechanisms of disease: Signaling pathways for cardiac hypertrophy and failure. N. Engl. J. Med. **341,** 1276–1283.

KAMISAGO, M., SHARMA, S.D., DE PALMA, S.R., SOLOMON, S., SHARMA, P., McDONOUGH, B., SMOOT, L., MULLEN, M., WOOLF, P.K., WIGLE, E., SEIDMAN, J.G., and SEIDMAN, C.E. (2000). Mutations in sarcomeric protein genes as a cause of dilated cardiomyopathy. N. Engl. J. Med. **343,** 1688–1696.

KROWN, K.A., PAGE, M.T., NGUYEN, C., ZECHNER, D., GUTIERREZ, V., COMSTOCK, K.L., GLEMBOTSKI, C.C., QUINTANA, P.J., and SABBADINI, R.A. (1996). Tumor necrosis factor α-induced apoptosis in cardiac myocytes. J. Clin. Invest. **98,** 2854–2865.

LAI, N.C., ROTH, D.M., GAO, M.H., FINE, S., HEAD, B.P., ZHU, J., McKIRNAN, M.D., KWONG, C., DALTON, N., URASAWA, K., ROTH, D.A., and HAMMOND, H.K. (2000). Intracoronary delivery of adenovirus encoding adenylyl cyclase VI increases left ventricular function and cAMP-generating capacity. Circulation **102,** 2396–2401.

LAUGWITZ, K.L., UNGERER, M., SCHÖNEBERG, T., WEIG, H.J., KRONSBEIN, K., MORETTI, A., HOFFMANN, K., SEYFARTH, M., SCHULTZ, G., and SCHÖMIG, A. (1999). Adenoviral gene transfer of the human V2 vasopressin receptor improves contractile force of rat cardiomyocytes. Circulation **99,** 925–933.

LERI, A., LIU, J., MALHOTRA, A., LI, Q., STIEGLER, P., CLAUDIO, P., GIORDANO, A., KAJSTURA, J., HINTZE, T., and ANVERSA P. (1998). Pacing-induced heart failure in dogs enhances the expression of p53 and p53-dependent genes in ventricular myocytes. Circulation **97,** 194–203.

MacLELLAN, W.R. (2000). Advances in the molecular mechanisms of heart failure. Curr. Opin. Cardiol. **15,** 128–135.

MASAKI, H., IMAIZUMI, T., ANDO, S., HIROOKA, Y., HARADA, S., MOMOHARA, M., NAGANO, M., and TAKESHITA, A. (1993). Production of chronic congestive heart failure by rapid ventricular pacing in the rabbit. Cardiovasc. Res. **27,** 828–831.

MASHIMA, T., NAITO, M., and TSURUO, T. (1999). Caspase-mediated cleavage of cytoskeletal actin plays a positive role in the process of morphological apoptosis. Oncogene **18,** 2423–2430.

MATSUI, T., LING, L., DEL MONTE, F., FUKUI, Y., FRANKE, T.H., HAJJAR, R.J., and ROSENZWEIG, A. (1999). Adenoviral gene transfer of activated phosphatidylinositol 3′-kinase and Akt inhibits apoptosis of hypoxic cardiomyocytes *in vitro*. Circulation **100,** 2373–2385.

NARULA, J., PANDEY, P., ARBUSTINI, E., HAIDER, N., NARULA, N., KOLODGIE, F.D., DAL BELLO, B., SEMIGRAN, M.J., BIELSA-MASDEU, A., DEC, G.W., ISRAELS, S., BALLESTER M., VIRMANI, R., SAXENA, S., and KHARBANDA, S. (1999). Apoptosis in heart failure: Release of cytochrome *c* from mitochondria and activation of caspase-3 in human cardiomyopathy. Proc. Natl. Acad. Sci. U.S.A. **96,** 8144–8149.

NICHOLSON, D.W. (2000). From bench to clinic with apoptosis-based therapeutic agents. Nature **407,** 810–816.

OLIVETTI, G., ABBI, R., QUAINI, F., KAJSTURA, J., CHENG, W., NITAHARA, J.A., QUAINI, E., DE LORETTO, C., BELTRAMI, C.A., KRAJEWSKI, S., REED, T.C., and ANVERSA, P. (1997). Apoptosis in the failing human heart. N. Engl. J. Med. **336,** 1131–1141.

REED, J.C., and PATERNOSTRO, G. (1999). Postmitochondrial regulation of apoptosis during heart failure. Proc. Natl. Acad. Sci. U.S.A. **96,** 7614–7616.

RUDEL, T., and BOKOCH, G.M. (1997). Membrane and morphological changes in apoptotic cells regulated by caspase-mediated activation of PAK2. Science **276,** 1571–1574.

SUN, H.Q., YAMAMOTO, M., MEJILLANO, M., and YIN, H.L. (1999). Gelsolin, a multifunctional actin regulatory protein. J. Biol. Chem. **274,** 33179–33182.

TOWBIN, J.A. (1998). The role of cytoskeletal proteins in cardiomyopathies. Curr. Opin. Cell. Biol. **10,** 131–139.

VILLA, P., KAUFMANN, S.H., and EARNSHAW, W.C. (1997). Caspases and caspase inhibitors. Trends Biochem. Sci. **22,** 388–393.

WEIG, H.J., LAUGWITZ, K.L., MORETTI, A., KRONSBEIN, K., STÄDELE, C., BRÜNING, S., SEYFARTH, M., BRILL, T., SCHÖMIG, A., and UNGERER, M. (2000). Enhanced cardiac contractility after gene transfer of V2 vasopressin receptors *in vivo* by ultrasound-guided injection or transcoronary delivery. Circulation **101,** 1578–1585.

Address reprint requests to:
Dr. Karl-Ludwig Laugwitz
I. Medizinische Klinik
Klinikum Rechts der Isar
Ismaninger Straße 22
D-81675 Munich, Germany

E-mail: laugwitz@med1.med.tu-muenchen.de

Received for publication May 9, 2001; accepted after revision October 11, 2001.

Published online: November 2, 2001.